# A Chance-Constrained Programming Framework to Handle Uncertainties in Radiation Therapy Treatment Planning

Maryam Zaghian[a], Gino J. Lim[b,*], Azin Khabazian[b]

[a]*Office of Performance Improvement, The University of Texas MD Anderson Cancer Center, 1515 Holocombe Blvd., Unit 0466, Houston, TX 77030, USA.*
[b]*Department of Industrial Engineering, University of Houston, 4800 Calhoun Road, Houston, TX 77204, USA.*

## Abstract

A stochastic programming framework is proposed for radiation therapy treatment planning. This framework takes into account uncertainty in setting up or positioning patients identically day-to-day during the treatment period. Because uncertainties are unavoidable, constraint violations are tolerated to some degree in practice. Under this assumption, a chance-constrained programming (CCP) framework is developed to handle setup uncertainties in treatment planning. The proposed framework can be employed under different distributional assumptions. The goal of the proposed approach is to maximize both the statistical confidence level of a treatment plan and the homogeneity of the dose distributions. This novel perspective provides a user-centric and personalized optimization model that allows a trade-off between sufficient tumor coverage and sparing healthy tissues under uncertainty. We describe testing of the performance of the proposed CCP models in terms of plan quality, robustness, and homogeneity and confidence level of the constraints using clinical data for a prostate cancer patient. Optimized CCP plans are also compared to plans developed using a deterministic approach that does not take uncertainties into account. Numerical experiments confirmed that the CCP is able to control setup uncertainties in target coverage and sparing of organs-at-risk.

*Keywords:* OR IN MEDICINE, CHANCE-CONSTRAINED PROGRAMMING, RADIATION TREATMENT PLANNING, SETUP UNCERTAINTY

*Corresponding author
    *Email addresses:* `mzaghian@mdanderson.org` (Maryam Zaghian), `ginolim@uh.edu` (Gino J. Lim ), `akhabazian@uh.edu` (Azin Khabazian)

## 1. Introduction

More than 1.6 million new cancer diagnoses and more than half a million cancer deaths are expected to occur in the United States in 2017, according to the American Cancer Society (Siegel et al., 2017). More than half of patients diagnosed with cancer undergo radiation therapy, some in conjunction with chemotherapy or surgery (American Cancer Society, 2015). Radiation therapy delivers radioactive particles to the tumor region in order to damage the DNA of the cells, interfering with their ability to divide and grow. An important goal in radiation therapy is to kill tumor cells while minimizing toxic effects on surrounding healthy tissues.

Two of the most advanced and common modalities of radiation therapy are intensity-modulated radiation therapy (IMRT) (Zelefsky et al., 2000, Lim, Choi, & Mohan, 2008, Lim and Cao, 2012), which uses photons, and intensity-modulated proton therapy (Lomax et al., 2001, Cao et al., 2013, 2014), which uses protons. In delivering radiation for therapy, both of the methods decompose one open beam into many "beamlets" for each angle. The intensity of each beamlet can be modulated to achieve the optimal treatment effect; hence, each beamlet can deliver a different level of radiation intensity. The goal in treatment planning is to find the optimal beamlet intensities that will deliver a dose distribution as close as possible to the radiation dose prescribed for treatment.

Several sources of uncertainty can degrade the outcome of radiation treatment. Setup error, a common source of uncertainty, affects the relative position of the tumor with respect to the treatment beams. Radiation therapy is often administered daily over a period of several weeks, and the patient needs to be set up on the treatment couch in the exact same position for each treatment. A change in position can cause the radiation dose received by a voxel (a three-dimensional unit of volume) to differ from the planned dose to that voxel.

One effective method for calculating tumor dose while minimizing the radiation exposure of healthy organs under conditions of uncertainty is robust optimization. Baum et al. (2006) highlighted the importance of robustness in radiation therapy. Olafsson and Wright (2006) presented a robust optimization approach simultaneously considering the uncertainties resulting from dose calculation and organ positions. Other researchers (Pflugfelder, Wilkens, & Oelfke, 2008, Liu et al., 2012b, Fredriksson, Forsgren, & Hårdemark, 2011) proposed using scenario-based worst-case robust optimization approaches. A further consideration in radiation treatment planning is that the optimization model should contain constraints to ensure clinical feasibility. However, some of the proposed robust optimization

models do not contain constraints (Pflugfelder, Wilkens, & Oelfke, 2008, Liu et al., 2012a, Fredriksson, Forsgren, & Hårdemark, 2011), which can result in infeasible solutions. When a solution is clinically infeasible, a planner must perform a post-processing remedial step to obtain a solution that eliminates or minimizes the constraint violations. We claim that information about clinical constraint violations under parameter uncertainties can help physicians decide whether the obtained solution is good enough to allow the treatment to proceed or whether an alternative treatment plan needs to be developed.

The clinical goal of achieving an effective dose for target tissue(s) while sparing the organs at risk (OARs) is often difficult to satisfy. Hence, some degree of clinical constraint violations can be tolerated by clinicians as long as the deviation is not too far from the clinical objective. This has motivated us to develop a probabilistic approach, specifically, a chance-constrained programming (CCP) model to address the problem using confidence levels. The underlying assumption of a chance-constrained framework is that we have full knowledge of the probability distribution of the uncertainty. Although we may not have enough data to infer the true probability distribution of an uncertain parameter, an approximate probability distribution of uncertainty can be included in the CCP framework.

CCP (Charnes and Cooper, 1959) has been widely studied and plays an important role in engineering, telecommunications, and finance (Geletu, Klöppel, & Li, 2013). Recently, An et al. (2017) presented a conditional value at risk (CVaR) chance-constrained treatment planning optimization in proton therapy. This stochastic programming technique assumes random data variations and allows constraint violations up to a specified tolerance level in the probabilistic setting. In general, CCP relaxes the constraints in a deterministic optimization model and replaces them with probabilistic constraints. Each chance constraint specifies the level of confidence for satisfying the corresponding deterministic constraint. Confidence levels can be helpful information for treatment planners because they allow treatment plans to be developed based on the decision maker's risk preference on constraint violation. Most of the existing treatment planning optimization models do not provide information about feasibility violation under uncertainty. For instance, in robust optimization, the goal is to achieve feasibility under any realization of a predetermined uncertainty set; however, in CCP, one seeks to satisfy the constraints with high probability. Nevertheless, for the special case of the ellipsoidal uncertainty set, chance constraints and deterministically robust constraints have been proven to be equivalent (Calafiore and El Ghaoui, 2006).

One of the limitations of the CCP approach is that the feasible set of a chance constraint

is usually nonconvex, which makes the optimization problem difficult to solve (Nemirovski and Shapiro, 2006). However, under some assumptions on an uncertain parameter, deterministic equivalent transformations have been developed (Charnes and Cooper, 1959, Geletu, Klöppel, & Li, 2013). Finding a feasible solution for the deterministic counterparts of the chance constraints is often computationally less burdensome than solving the original stochastic model.

Therefore, in this paper, a CCP framework is developed to optimize radiation therapy treatment plans under conditions of uncertainty regarding the patient setup. The proposed model controls the frequency of constraint violations and provides optimized treatment plans along with a corresponding confidence level. A confidence level, the probability that the constraints will hold under uncertainties, can help the physician to select an appropriate treatment plan based on the risk tolerance level for constraint violation. We first construct the chance-constrained framework to control the dose to each anatomical structure by addressing the clinical requirements for treatment: controlling the cold spots and hot spots on the target while sparing normal tissues. (A cold spot is a portion of tissue that receives less than the desired radiation dose, and a hot spot is a portion of tissue that receives a dose higher than the desired dose.) The practical application of CCP necessitates a rational method for choosing risk levels or tolerances for the chance constraints; this issue is addressed by optimizing the confidence levels within the proposed framework. However, if the confidence levels are implicitly known as part of the decision process, the framework can help to maximize the homogeneity of the dose distributions. In addition, we derive second-order cone programming equivalents of the chance constraints and employ the framework to handle uncertainties under different probability distributions.

This paper makes three main contributions. (1) A chance-constrained optimization framework is developed to handle random setup uncertainties in the problem of radiation therapy treatment planning. (2) Within the framework of CCP, confidence levels (i.e., the probability of satisfying the constraints) and the plan's quality, robustness, and homogeneity are optimized. (3) We demonstrate that the CCP framework can be extended to an uncertainty with a specific probability distribution with simple modification.

The paper is organized into 5 sections. The problem and the notation for the problem formulation are described in Section 2. CCP is defined in a general setting in Section 3. We add an explanation about how chance constraints for radiation therapy treatment planning and the corresponding CCP framework can be constructed. The extension of this framework for different uncertainties with specific probability distributions is also

4

elaborated in Section 3. Section 4 discusses the results of a case study using clinical data from a patient with prostate cancer. We offer our conclusions in Section 5.

## 2. Problem Description and Notation

The goal of a fluence map optimization in radiation therapy treatment planning is to find the optimal beamlet weights, the amount of radiation that each beamlet delivers when the gantry is positioned at a given angle. The deterministic fluence map optimization model we use in this paper is presented in Lim, Choi, & Mohan (2008).

The input parameters for radiation therapy treatment planning models are shown in Table 1.

Table 1: Parameter definition

| | |
|---|---|
| T | A set of voxels in the clinical target volume |
| OAR | A set of voxels in organs-at-risk |
| J | A set of all beamlets |
| $\theta_L$ | Cold-spot control parameter on target |
| $\theta_U$ | Hot-spot control parameter on target |
| $\varphi$ | Hot-spot control parameter on OAR |
| $\lambda_T^+$ | Penalty coefficient for hot spots on target |
| $\lambda_T^-$ | Penalty coefficient for cold spots on target |
| $\lambda_{OAR}$ | Penalty coefficient for hot spots on OAR |
| $\alpha_T^+$ | Risk level for having cold spots on target |
| $\alpha_T^-$ | Risk level for having hot spots on target |
| $\alpha_{OAR}^+$ | Risk level for having hot spots on OAR |

Given that the decision variable $w_j$ is the intensity of beamlet $j \in J$, the total dose in voxel $i$ can be calculated as

$$D_i(w) = \sum_{j \in J} d_{ij} w_j, \ \forall i \in \{T \cup OAR\},$$

where $d_{ij}$ denotes the dose contributed by the $j^{th}$ beamlet per unit weight and received by voxel $i$. In a matrix format, we have

$$D_i(w) = d_i^T w,$$

5

where $d_i$ represents the dose contribution from all beamlets to voxel $i$ and $w$ is the intensity vector of the beamlets.

## 3. Chance-constrained programming

Let us consider the following problem:

$$\{x|(\varepsilon : A_i(\varepsilon)x \geq b_i(\varepsilon))\}, \tag{1}$$

where $x \in R^n$ is the decision variable and $\varepsilon$ is a random variable affecting both $A_i$ and $b_i$ for all $i = 1, \ldots, m$. A classical approach to the solution of (1) under random uncertainty is to introduce risk levels $\alpha_i$ for $i = 1, \ldots, m$ and to enforce the constraints satisfied with, at most, probability $(1 - \alpha_i)$, in any choice of $x$, thus obtaining the so-called CCP. A generic form of chance constraints can be stated as:

$$\{x|\varepsilon : P[A_i(\varepsilon)x \geq b_i(\varepsilon)] \geq 1 - \alpha_i\} \qquad i = 1, \ldots, m \tag{2}$$

In the following section, constraint (2) is used to construct chance constraints for radiation therapy treatment planning optimization under patient setup uncertainty.

### 3.1. Chance-constraints for treatment planning

Under a setup uncertainty, the random dose delivered to voxel $i$ is denoted by

$$\tilde{D}_i(w) = \tilde{d}_i^T w, \ \forall i \in \{T \cup OAR\},$$

where $\tilde{d}_i$ is a random variable that denotes the amount of radiation dose received in voxel $i$ by all beamlets with a unit intensity (or weight).

Under the nominal assumption (i.e., no uncertainty), the target must receive a dose over $\theta_L$, a lower threshold value on the target:

$$D_T(w) \geq \theta_L, \tag{3}$$

where $D_T(w)$ is essentially the same as $\tilde{D}_T(w)$. However, constraint (3) becomes (4) under uncertainty:

$$\tilde{D}_T(w) \geq \theta_L \tag{4}$$

6

We reformulate this constraint as a chance-constrained framework by introducing a confidence level and enforcing the constraint with probability, as represented in (5).

$$P\{\tilde{D}_T(w) \geq \theta_L\} \geq 1 - \alpha_T^-, \tag{5}$$

where $1 - \alpha_T^-$ is the confidence level for avoiding cold spots on target voxels.

In addition, the dose received by a target voxel is limited to some level $\theta_U$ in order to minimize hot spots on the tumor. The corresponding deterministic constraint is shown in (6).

$$D_T(w) \leq \theta_U \tag{6}$$

In a stochastic framework, constraint (6) can be written as

$$\tilde{D}_T(w) \leq \theta_U, \tag{7}$$

and the probabilistic representation of constraint (7) is

$$P\{\tilde{D}_T(w) \leq \theta_U\} \geq 1 - \alpha_T^+, \tag{8}$$

where $1 - \alpha_T^+$ is the confidence level for limiting hot spots on target voxels.

Similarly, chance constraints can be defined for OAR sparing. If a voxel belongs to a healthy structure or an OAR, it is desirable to limit the dose below some level $\varphi$, which is a structure-specific parameter. Equations (9), (10), and (11) are the OAR-sparing constraints in the format of deterministic, stochastic, and chance constraints, respectively.

$$D_{OAR}(w) \leq \varphi \tag{9}$$

$$\tilde{D}_{OAR}(w) \leq \varphi \tag{10}$$

$$P\{\tilde{D}_{OAR}(w) \leq \varphi\} \geq 1 - \alpha_{OAR}^+, \tag{11}$$

where $1 - \alpha_{OAR}^+$ is the confidence level for the sparing of voxels in OAR. Note that there are often more than one OAR structure is located in a treatment site.

The following two remarks highlight the feasibility of chance constraints when compared to deterministic and stochastic constraints:

**Remark 1.** Any of the chance constraints (5), (8), or (11) are feasible if the corresponding

deterministic constraints (3), (6), or (9) are feasible.

**Remark 2.** Any feasible solution of the stochastic constraints (4), (7), or (10) is feasible for the corresponding chance constraints (5), (8), or (11).

*3.2. CCP models under normal distribution (CCP-N)*

In this section, the dose contribution vector $\tilde{d}_i$ is assumed to be normally distributed with mean $E(\tilde{d}_i)$ and standard deviation $\sigma(\tilde{d}_i)$ (Fredriksson, Forsgren, & Hårdemark, 2015). The normal probability distribution has attractive analytical properties that facilitate further analysis (Chan, Tsitsiklis, & Bortfeld, 2010). Furthermore, the sum of the random errors with arbitrary distributions will converge to a normal distribution, as follows from a central limit theorem. Hence, the normality assumption will also help to extend the analysis for multiple sources of uncertainty (Chu et al., 2005).

It should be noted that one of the difficulties in solving this probabilistically constrained model comes from the fact that the chance constraints (5), (8), or (11) may not be convex (Nemirovski and Shapiro, 2006). Under the normality assumption of uncertainty, we can prove that these constraints are convex. Thus, the optimization model becomes easier to solve. Proposition 1 and Corollary 1 below elaborate the convexity of the treatment planning chance constraints under the assumption of normal distribution for uncertainties. Then, Proposition 2 provides linear deterministic equivalents of the chance constraints (5), (8), and (11).

**Proposition 1.** Assuming that an uncertain parameter follows a normal distribution, the feasible region for each of the chance constraints (5), (8), or (11) is convex for any $\alpha \leq 1/2$.

*Proof.* Suppose the uncertain coefficients $\tilde{d}_i, \forall i = 1, \cdots,$ depend affinely on a random variable $\tilde{\epsilon}_{ij}$ whose distributions are normal, so we have

$$d_i(\tilde{\epsilon}) = d_i^0 + \sum_{j \in J} d_i^j \tilde{\epsilon}_{ij},$$

where $d_i^0$ vector is equal to $E(\tilde{d}_i)$, and elements of $d_i^j$ vectors are 0 except for the $j^{th}$ element which is 1. Under the affine dependence of uncertainties on the random vector, the chance

constraints (5), (8), or (11) are of the forms (12) - (14), respectively.

$$P\{\tilde{D}_T(w) \geq \theta_L\} = P\{-(d_T^0 + \sum_{j \in J} d_T^j \tilde{\epsilon}_{Tj})^T w \leq -\theta_L\} \geq 1 - \alpha_T^- \qquad (12)$$

$$P\{\tilde{D}_T(w) \leq \theta_U\} = P\{(d_T^0 + \sum_{j \in J} d_T^j \tilde{\epsilon}_{Tj})^T w \leq \theta_U\} \geq 1 - \alpha_T^+ \qquad (13)$$

$$P\{\tilde{D}_{OAR}(w) \leq \varphi\} = P\{(d_{OAR}^0 + \sum_{j \in J} d_{OAR}^j \tilde{\epsilon}_{OARj})^T w \leq \theta_U\} \geq 1 - \alpha_{OAR}^+, \qquad (14)$$

where (12) - (14) have the same form as $P\{(a_0 + \tilde{a})^T x \leq b\} \leq 1 - \alpha$. It is known that any chance-constrained linear program of the form

$$\max \quad c^T x$$
$$s.t.$$
$$P\{(a_0 + \tilde{a})^T x \leq b\} \leq 1 - \alpha,$$

with the acceptable risk level $\alpha \leq 1/2$ is a convex program, if the distribution of uncertain parameter $\tilde{a}$ is log-concave and symmetric (Nemirovski and Shapiro, 2006, Prékopa, 1995). Since $\tilde{\epsilon}$ is assumed to be normally distributed, and normal distributions have a log-concave symmetric density function, the feasible region for any of the chance constraints (5), (8), or (11) is convex. $\qquad \square$

**Corollary 1.** Consider the system of chance constraints (15) for the problem of treatment planning optimization. The feasible region for the set of chance constraints (15) is convex for any $\alpha \leq 1/2$ under the assumption of normal distribution for uncertainties.

$$P\{\tilde{D}_T(w) \geq \theta_L\} \geq 1 - \alpha_T^- \qquad \forall T \qquad (15)$$
$$P\{\tilde{D}_T(w) \leq \theta_U\} \geq 1 - \alpha_T^+ \qquad \forall T$$
$$P\{\tilde{D}_{OAR}(w) \leq \varphi\} \geq 1 - \alpha_{OAR}^+ \qquad \forall OAR$$

*Proof.* According to Proposition 1, the feasible region of any individual constraint in (15) is convex for any $\alpha \leq 1/2$ under the assumption of normal distribution for uncertainty. It is known that the intersection of convex sets is convex (Bazaraa, Sherali, & Shetty, 2013). As a result, the feasible region of (15) is convex. $\qquad \square$

**Proposition 2.** Let random dose $\tilde{D}_i(w)$ follow a normal distribution with mean $E(\tilde{D}_i(w))$ and standard deviation $\sigma(\tilde{D}_i(w))$, and consider the following set of constraints:

$$\mathbf{E}(\tilde{D}_T(w)) - \Phi^{-1}(1 - \alpha_T^-)\sigma(\tilde{D}_T(w)) \geq \theta_L \qquad \forall\, T \tag{16}$$

$$\mathbf{E}(\tilde{D}_T(w)) + \Phi^{-1}(1 - \alpha_T^+)\sigma(\tilde{D}_T(w)) \leq \theta_U \qquad \forall\, T \tag{17}$$

$$\mathbf{E}(\tilde{D}_{OAR}(w)) + \Phi^{-1}(1 - \alpha_{OAR}^+)\sigma(\tilde{D}_{OAR}(w)) \leq \varphi \quad \forall\, OAR \tag{18}$$

Then, every feasible solution of the constraints (16)-(18) is feasible for the constraint (15), where $\Phi(\cdot)$ represents the cumulative distribution of a normal standard probability density.

*Proof.* Under the normality assumption of $\tilde{D}_i(w)$, the standardized form of $\tilde{D}_i(w)$ is defined as

$$\tilde{Z}_i(w) = \frac{\tilde{D}_i(w) - \mathbf{E}(\tilde{D}_i(w))}{\sigma(\tilde{D}_i(w))}$$

In order to yield the desired result for the constraint (16), the chance constraint (5) can be transformed by simple subtraction and division as follows:

$$P\{\frac{\tilde{D}_T(w) - \mathbf{E}(\tilde{D}_T(w))}{\sigma(\tilde{D}_T(w))} \geq \frac{\theta_L - \mathbf{E}(\tilde{D}_T(w))}{\sigma(\tilde{D}_T(w))}\} \geq 1 - \alpha_T^-$$

$$P\{\tilde{Z}_T(w) \leq \frac{\theta_L - \mathbf{E}(\tilde{D}_T(w))}{\sigma(\tilde{D}_T(w))}\} \leq \alpha_T^-$$

$$\frac{\theta_L - \mathbf{E}(\tilde{D}_T(w))}{\sigma(\tilde{D}_T(w))} \leq \Phi^{-1}(\alpha_T^-),$$

from which constraint (16) is obtained.

Next, we derive the deterministic equivalent of the chance constraint (8).

$$P\{\frac{\tilde{D}_T(w) - \mathbf{E}(\tilde{D}_T(w))}{\sigma(\tilde{D}_T(w))} \leq \frac{\theta_U - \mathbf{E}(\tilde{D}_T(w))}{\sigma(\tilde{D}_T(w))}\} \geq 1 - \alpha_T^+$$

$$P\{\tilde{Z}_T(w) \leq \frac{\theta_U - \mathbf{E}(\tilde{D}_T(w))}{\sigma(\tilde{D}_T(w))}\} \geq 1 - \alpha_T^+$$

$$\frac{\theta_U - \mathbf{E}(\tilde{D}_T(w))}{\sigma(\tilde{D}_T(w))} \geq \Phi^{-1}(1 - \alpha_T^+),$$

10

from which constraint (17) follows. In a similar fashion, it can be shown that constraint (18) is equivalent to (11). □

The dose calculated using any feasible solution of the constraints (16)-(18) will be within the lower- and upper-boundary control parameters prescribed for each structure with the specified confidence level for each voxel. Typically, the same dose is prescribed to all voxels in the target, so we assume equal confidence levels for all voxels in the same structure for each set of constraints. In other words, the resulting dose of any feasible solution of constraints (16)-(18) is greater than $\theta_L$ with confidence level $(1 - \alpha_T^-)\%$ and less than $\theta_U$ with confidence level $(1 - \alpha_T^+)\%$ for each target voxel, and also less than $\varphi$ with confidence level $(1 - \alpha_{OAR}^+)\%$ for each OAR voxel, in the face of uncertainty.

*3.2.1. CCP-N (I)*

In this section, we develop a model in which the confidence levels $(1-\alpha)$ described above become decision variables, leading to a formulation (19) that maximizes the confidence levels $(1 - \alpha)$ for all voxels.

$$\max \quad \lambda_T^-(1 - \alpha_T^-) + \lambda_T^+(1 - \alpha_T^+) + \lambda_{OAR}(1 - \alpha_{OAR}^+) \tag{19}$$

$$s.t.$$

$$\mathbf{E}(\tilde{D}_T(w)) - \Phi^{-1}(1 - \alpha_T^-)\sigma(\tilde{D}_T(w)) \geq \theta_L \qquad \forall T$$

$$\mathbf{E}(\tilde{D}_T(w)) + \Phi^{-1}(1 - \alpha_T^+)\sigma(\tilde{D}_T(w)) \leq \theta_U \qquad \forall T$$

$$\mathbf{E}(\tilde{D}_{OAR}(w)) + \Phi^{-1}(1 - \alpha_{OAR}^+)\sigma(\tilde{D}_{OAR}(w)) \leq \varphi \quad \forall OAR$$

$$\alpha_T^-, \alpha_T^+, \alpha_{OAR}^+ \leq 1/2$$

$$w \geq 0,$$

where $\lambda_T^-$, $\lambda_T^+$, and $\lambda_{OAR}$ are penalty coefficients for cold spots on the target, hot spots on the target, and hot spots on the OAR, respectively.

However, the inverse function $\Phi^{-1}(y)$ makes it difficult to find the optimal value of $\alpha$ in model (19). Instead, the model can be reformulated as

$$\max \quad \lambda_T^- \, \Phi^{-1}(1 - \alpha_T^-) + \lambda_T^+ \, \Phi^{-1}(1 - \alpha_T^+) + \lambda_{OAR} \, \Phi^{-1}(1 - \alpha_{OAR}^+) \tag{20}$$

$$s.t.$$

$$Constraints \ of \ model \ (19),$$

because $\Phi^{-1}(y)$ is a monotonically increasing function of $y$. Considering $\Phi^{-1}(1-\alpha) = G_\alpha$ as a new set of variables for $\alpha \in \{\alpha_T^-, \alpha_T^+, \alpha_{OAR}^+\}$, the model is simplified as follows:

$$\max \quad \lambda_T^- \, G_{(\alpha_T^-)} + \lambda_T^+ \, G_{(\alpha_T^+)} + \lambda_{OAR} \, G_{(\alpha_{OAR}^+)} \tag{21}$$

$$s.t.$$

$$\mathbf{E}(\tilde{D}_T(w)) - G_{(\alpha_T^-)} \, \sigma(\tilde{D}_T(w)) \geq \theta_L \qquad \forall T$$

$$\mathbf{E}(\tilde{D}_T(w)) + G_{(\alpha_T^+)} \, \sigma(\tilde{D}_T(w)) \leq \theta_U \qquad \forall T$$

$$\mathbf{E}(\tilde{D}_{OAR}(w)) + G_{(\alpha_{OAR}^+)} \, \sigma(\tilde{D}_{OAR}(w)) \leq \varphi \quad \forall OAR$$

$$G_{\alpha_T^-}, G_{\alpha_T^+}, G_{\alpha_{OAR}^+} \geq 0$$

$$w \geq 0.$$

### 3.2.2. CCP-N (II)

In some situations, the treatment planner may wish to develop a plan that satisfies a preferred value of confidence $(\alpha_.)$. This level of confidence may violate constraint feasibility for fixed values of $\theta_L, \theta_U$, and $\varphi$; hence, these three parameters can be treated as variables. Then, an optimization model can be developed to find optimal beamlet intensities in such a way that deviations of these three variables from their target values can be minimized, i.e., $min\ (\theta_U - \theta_L)$ and $min\ \varphi$ for a given level of confidence $(1-\alpha_.)$. Therefore, we propose the following optimization model (22), in which $\theta_L, \theta_U$, and $\varphi$ are considered as decision variables for a fixed value $\alpha_.$ for each organ.

$$\min \quad -\lambda_T^- \, \theta_L + \lambda_T^+ \, \theta_U + \lambda_{OAR}^+ \, \varphi \tag{22}$$

$$s.t.$$

$$\mathbf{E}(\tilde{D}_T(w)) - \Phi^{-1}(1-\alpha_T^-)\sigma(\tilde{D}_T(w)) \geq \theta_L \qquad \forall T$$

$$\mathbf{E}(\tilde{D}_T(w)) + \Phi^{-1}(1-\alpha_T^+)\sigma(\tilde{D}_T(w)) \leq \theta_U \qquad \forall T$$

$$\mathbf{E}(\tilde{D}_{OAR}(w)) + \Phi^{-1}(1-\alpha_{OAR}^+)\sigma(\tilde{D}_{OAR}(w)) \leq \varphi \quad \forall OAR$$

$$\underline{\theta}_L \leq \theta_L \leq \bar{\theta}_L$$

$$\underline{\theta}_U \leq \theta_U \leq \bar{\theta}_U$$

$$\varphi, w \geq 0$$

where $\underline{\theta}$ and $\bar{\theta}$ are lower and upper bounds for variables $\theta$, respectively.

*3.3. CCP models under uniform distribution (CCP-U)*

In this section, the vector $\tilde{d}_i - \mathbf{E}(\tilde{d}_i)$ is assumed to be uniformly distributed in the ellipsoid $\varepsilon = \{\xi = Qz : \|z\| \leq 1\}$ where $Q = \upsilon\Gamma_f, \Gamma = \sigma^2(\tilde{d}_i) \succ 0, \upsilon = \sqrt{n+3}, \Gamma_f \in R^n$, and $\upsilon$ is a full rank factor such that $\Gamma = \Gamma_f\Gamma_f^T$. Under a uniform distributional assumption for uncertainties, Proposition 3 and Corollary 2 below explore the convexity of the treatment planning chance constraints. Those are followed by Proposition 4, which is related to the work by Calafiore and El Ghaoui (2006) and provides deterministic linear equivalents of the chance constraints (15) under the above-mentioned assumptions.

**Proposition 3.** For any $\alpha \leq 1/2$, the feasible region for each of the chance constraints (5), (8), or (11) is convex, if uncertain dose distributions $\tilde{d}_i - \mathbf{E}(\tilde{d}_i)$ are uniformly distributed in the ellipsoid $\varepsilon = \{\xi = Qz : \|z\| \leq 1\}$.

*Proof.* Assume uncertain coefficients $\tilde{d}_i$ depend affinely on a random vector $\tilde{\epsilon}_{ij}$. Uniformly distributed $\tilde{d}_i - \mathbf{E}(\tilde{d}_i)$ is defined as

$$\tilde{d}_i - \mathbf{E}(\tilde{d}_i) = d_i(\tilde{\epsilon}) - d_i^0 = \sum_{j \in J} d_i^j \tilde{\epsilon}_{ij}.$$

The proof follows in similar fashion to the proof of Proposition 1. Under the above-mentioned assumptions, the chance constraints (5), (8), or (11) are of the forms (12), (13), or (14), respectively.
It is assumed that $\sum_{j \in J} d_i^j \tilde{\epsilon}_{ij}$ follows a uniform distribution in the ellipsoid $\varepsilon = \{\xi = Qz : \|z\| \leq 1\}$, which has a log-concave distribution function. Hence, the feasible region for any of the chance constraints (5), (8), or (11) is convex (Nemirovski and Shapiro, 2006, Prékopa, 1995). $\square$

**Corollary 2.** *For any risk level $\alpha \leq 1/2$, the feasible region of the set of chance constraints (15) is convex if $\tilde{d}_i - \mathbf{E}(\tilde{d}_i)$ is uniformly distributed in the ellipsoid $\varepsilon = \{\xi = Qz : \|z\| \leq 1\}$.*

*Proof.* From Proposition 3, we know that for any $\alpha \leq 1/2$, the feasible region of any individual constraint in (15) is a convex set if vector $\tilde{d}_i - \mathbf{E}(\tilde{d}_i)$ is uniformly distributed in the ellipsoid $\varepsilon = \{\xi = Qz : \|z\| \leq 1\}$. Similar to the proof of Corollary 1, this extension is the consequence of the fact that the intersection of convex sets is still convex (Bazaraa, Sherali, & Shetty, 2013). Therefore, we can conclude that the feasible region of (15) is convex if the assumptions hold. $\square$

**Proposition 4.** Assume $\tilde{d}_i - \mathbf{E}(\tilde{d}_i)$ is uniformly distributed in the ellipsoid set $\varepsilon = \{\xi = Qz : \|z\| \leq 1\}$, in which $Q = v\Gamma_f$ $v = \sqrt{n+3}$, and consider the following set of constraints:

$$\mathbf{E}(\tilde{D}_T(w)) - v\sqrt{\Psi_{beta}^{-1}(1 - 2\alpha_T^-)}\,\sigma(\tilde{D}_T(w)) \geq \theta_L \qquad\qquad \forall\, T \qquad\qquad (23)$$

$$\mathbf{E}(\tilde{D}_T(w)) + v\sqrt{\Psi_{beta}^{-1}(1 - 2\alpha_T^+)}\,\sigma(\tilde{D}_T(w)) \leq \theta_U \qquad\qquad \forall\, T \qquad\qquad (24)$$

$$\mathbf{E}(\tilde{D}_{OAR}(w)) + v\sqrt{\Psi_{beta}^{-1}(1 - 2\alpha_{OAR}^+)}\,\sigma(\tilde{D}_{OAR}(w)) \leq \varphi \qquad \forall OAR \qquad (25)$$

Then, for any $\alpha \in (0, 0.5]$, every feasible solution of the constraints (23)-(25) is feasible for the chance constraints (5), (8), and (11), respectively. $\Psi_{beta}(\cdot)$ is the cumulative distribution function (CDF) of a $beta(1/2; n/2 + 1)$ probability density function (PDF).

*Proof.* Consider the chance-constrained set (15). By subtracting $\mathbf{E}(\tilde{D}_i(w))$ from each side of the constraints inside the probability, we can reformulate the constraints to

$$P\Big\{\frac{\tilde{D}_T(w) - \mathbf{E}(\tilde{D}_T(w))}{\sigma(\tilde{D}_T(w))} \geq \frac{\theta_L - E(\tilde{D}_T(w))}{\sigma(\tilde{D}_T(w))}\Big\} \geq 1 - \alpha_T^- \qquad\qquad (26)$$

$$P\Big\{\frac{\tilde{D}_T(w) - \mathbf{E}(\tilde{D}_T(w))}{\sigma(\tilde{D}_T(w))} \geq \frac{\theta_U - E(\tilde{D}_T(w))}{\sigma(\tilde{D}_T(w))}\Big\} \geq 1 - \alpha_T^+ \qquad\qquad (27)$$

$$P\Big\{\frac{\tilde{D}_{OAR}(w) - \mathbf{E}(\tilde{D}_{OAR}(w))}{\sigma(\tilde{D}_{OAR}(w))} \geq \frac{\varphi - E(\tilde{D}_{OAR}(w))}{\sigma(\tilde{D}_{OAR}(w))}\Big\} \geq 1 - \alpha_{OAR}^+. \qquad (28)$$

Since the vector $\tilde{d}_i - \mathbf{E}(\tilde{d}_i)$ is uniform in $\varepsilon$, we have

$$\tilde{d}_i - \mathbf{E}(\tilde{d}_i) = v\Gamma_f h, \qquad\qquad (29)$$

where $h \in R^{n+1}$ is uniform in $\{z : \|z\| \leq 1\}$. By applying (29), we will obtain

$$\tilde{D}_i(w) - \mathbf{E}(\tilde{D}_i(w)) = (v\Gamma_f h)^T w.$$

According to Calafiore and El Ghaoui (2006), the distribution function of $[\tilde{D}_i(w) - \mathbf{E}(\tilde{D}_i(w))]/v\sigma(\tilde{D}_i(w))$ is

$$\frac{nV_n}{nV_{n+1}}(1 - \xi^2)^{n/2}, \xi \in [-1, 1],$$

in which $V_n$ is

$$V_n = \frac{\pi^{n/2}}{\Gamma(n/2+1)}.$$

In order to prove the inequality (23), it is sufficient to show that CDF $\Psi(\xi), \xi \in [-1,1]$, is given by

$$\Psi(\xi) = 1/2 + (1/2)sign(\xi) \int_0^{|\xi|} (2\frac{nV_n}{nV_{n+1}})(1-x^2)^{n/2}dx. \tag{30}$$

With the change of variable $z = x^2$, the equation (30) can be written as follows

$$\Psi(\xi) = 1/2 + (1/2)sign(\xi)\Psi_{beta}(\xi^2),$$

where $\Psi_{beta}$ denotes the CDF of a beta(1/2;n/2+1) PDF.
Considering (26), we have

$$\Psi\{[\theta_L - \mathbf{E}(\tilde{D}_T^-(w))]/\upsilon\sigma(\tilde{D}_T^-(w))\} \geq \alpha_T^-.$$

By substituting $\Psi(.)$, we have

$$1/2 + (1/2)sign(M_T^-)\Psi_{beta}(M_T^{-2}) \geq \alpha_T^-,$$

where $M_T^- = \{[\theta_L - \mathbf{E}(\tilde{D}_T^-(w))]/\upsilon\sigma(\tilde{D}_T^-(w))\}$. Hence,

$$sign(M_T^-)\Psi_{beta}(M_T^{-2}) \geq 2\alpha_T^- - 1$$

It follows that

$$\{\frac{\theta_L - \mathbf{E}(\tilde{D}_T^-(w))}{\upsilon\sigma(\tilde{D}_T^-(w))}\}^2 \geq \Psi_{beta}^{-1}(1 - 2\alpha_T^-),$$

which yields

$$\mathbf{E}(\tilde{D}_T^-(w)) + \upsilon\sqrt{\Psi_{beta}^{-1}(1 - 2\alpha_T^-)}\sigma(\tilde{D}_T^-(w)) \leq \theta_L.$$

This inequality completes the proof for equation (23). Similarly, constraints (24) and (25)

15

can be expressed following the process shown above. □

### 3.3.1. CCP-U (I)

In order to maximize the confidence level of treatment plans, the objective function of model (19) is imposed on constraints (23)-(25). The resulting model can be reformulated as shown in model (31) because $\Psi_{beta}^{-1}(y)$ is a monotonically increasing function of $y$.

$$\max \quad \lambda_T^- k_{(\alpha_T^-)} + \lambda_T^+ k_{(\alpha_T^+)} + \lambda_{OAR} k_{(\alpha_{OAR}^+)} \tag{31}$$

$$s.t.$$

$$\mathbf{E}(\tilde{D}_T(w)) - \sqrt{k_{(\alpha_T^-)}}\, \sigma(\tilde{D}_T(w)) \geq \theta_L \qquad \forall\, T$$

$$\mathbf{E}(\tilde{D}_T(w)) + \sqrt{k_{(\alpha_T^+)}}\, \sigma(\tilde{D}_T(w)) \leq \theta_U \qquad \forall\, T$$

$$\mathbf{E}(\tilde{D}_{OAR}(w)) + \sqrt{k_{(\alpha_{OAR}^+)}}\, \sigma(\tilde{D}_{OAR}(w)) \leq \varphi \qquad \forall\, OAR$$

$$k_{\alpha_T^-}, k_{\alpha_T^+}, k_{\alpha_{OAR}^+} \geq 0$$

$$w \geq 0,$$

where $k_\alpha = v^2 \Psi_{beta}^{-1}(1 - 2\alpha)$ for $\alpha \in \{\alpha_T^-, \alpha_T^+, \alpha_{OAR}^+\}$.

### 3.3.2. CCP-U (II)

It is known that the confidence for the solution of beamlet intensities is inversely proportional to the tightness of the constraints. The larger $\theta_L$ and the smaller $\theta_U$ and $\varphi$ are, the tighter the constraint is. Model (32) is developed to optimize the thresholds of the constraints with a pre-specified probability. The logic behind this model is similar to that of model (22) explained in Section 3.2.2, but proposed here under the uniform distributional

16

assumption of uncertainties.

$$\min \quad -\lambda_T^- \theta_L + \lambda_T^+ \theta_U + \lambda_{OAR}^+ \varphi \qquad\qquad (32)$$

$$s.t.$$

$$\mathbf{E}(\tilde{D}_T(w)) - \upsilon\sqrt{\Psi_{beta}^{-1}(1 - 2\alpha_T^-)}\,\sigma(\tilde{D}_T(w)) \geq \theta_L \qquad\qquad \forall\, T$$

$$\mathbf{E}(\tilde{D}_T(w)) + \upsilon\sqrt{\Psi_{beta}^{-1}(1 - 2\alpha_T^+)}\,\sigma(\tilde{D}_T(w)) \leq \theta_U \qquad\qquad \forall\, T$$

$$\mathbf{E}(\tilde{D}_{OAR}(w)) + \upsilon\sqrt{\Psi_{beta}^{-1}(1 - 2\alpha_{OAR}^+)}\,\sigma(\tilde{D}_{OAR}(w)) \leq \varphi \qquad \forall\, OAR$$

$$\underline{\theta}_L \leq \theta_L \leq \bar{\theta}_L$$

$$\underline{\theta}_U \leq \theta_U \leq \bar{\theta}_U$$

$$\varphi, w \geq 0$$

## 4. Experiments and results

### 4.1. Clinical example

Data from one patient with prostate cancer treated at The University of Texas MD Anderson Cancer Center were used to illustrate the results of the proposed CCP models. Target volume and normal structures were manually contoured on the axial slices of the planning computed tomography scan by a physician. The anatomy was discretized into voxels of size 2.5 mm $\times$ 2.5 mm $\times$ 2.5 mm. Treatments were delivered using six fixed coplanar photon beams at angles of $30°, 90°, 120°, 150°, 240°$, and $270°$. These angles were given *a priori* as input to the optimization model. A prescription dose of 76 Gy was used for treatment planning.

Because our study focused on treatment planning considering a random setup error, we set up the experiment using two possible maximum shift positions from the original position of the patient (nominal position): $\pm 5$ and $\pm 7.5$ mm. In the case of a $\pm 5$ mm shift, five scenarios $(0, \pm 2.5$ mm, and $\pm 5$ mm) were considered. Without loss of generality, the data were generated by sampling from a probability distribution of a random error, specifically, normal and uniform distributions. Similarly, seven scenarios were constructed in the case of $\pm 7.5$ mm setup error. Then, the first and second order moments of the corresponding random dose distributions were calculated. Using the statistical information, treatment plans were developed and the deterministic (nominal) and CCP models were compared in terms of plan quality and robustness, confidence level, and homogeneities.

## 4.2. Plan quality and robustness

In this section, the quality and robustness of plans developed by deterministic and CCP models are compared. For the sake of comparison, all plans were renormalized to have at least 95% of target covered by the prescribed dose, which is a common practice at MD Anderson. Dose-volume indices ($D_v$ and $V_d$) were used to evaluate the quality of the plans, where $D_v$ denotes the amount of dose received by more than $v$ percent of the organ, and $V_d$ denotes the percentage of the organ volume receiving dose of more than $d$ Gy.

A dose-volume histogram (DVH) is a quantitative tool for assessing the appropriateness of a given radiation therapy plan (Drzymala et al., 1991). To compare the robustness of plans generated using different methods, families of DVHs corresponding to different setup scenarios were plotted along with the nominal DVH. The resulting envelopes were used to assess the sensitivity of the plans under the uncertainties. However, evaluation and comparison of the robustness of different methods using the envelope may not be accurate enough, so the DVH family band width method (Trofimov et al., 2012) was used. The width of the DVH band ($\Delta$) is inversely proportional to the robustness of the method. Here, $\Delta(D_v)$ denotes the width of the DVH band at volume $v$, and $\Delta(V_d)$ denotes the width of the DVH band at dose $d$. This robustness evaluation technique effectively determines the robustness of the plans in the presence of uncertainty.

In Figures 1 and 2, the DVHs corresponding to the nominal dose distribution are displayed along with the DVH bands for the deterministic and chance-constrained models. Target coverage and OAR sparing provided by nominal plans were clinically acceptable for all plans. However, the target coverage provided by the plan based on the deterministic model was notably less robust than the target coverage of the plans generated using chance-constrained models. The DVH bands for the target were wider for the deterministic plan than for those of the chance-constrained models, indicating that CCP outperformed the deterministic model under setup uncertainty. In addition, the robustness of plans created using CCP models under two different distributional assumptions was similar. Both the deterministic model and the CCP approach were similarly robust in regard to normal tissue sparing.
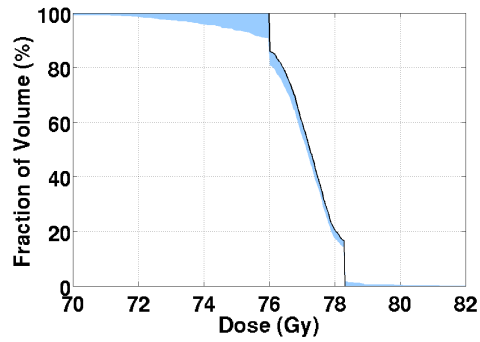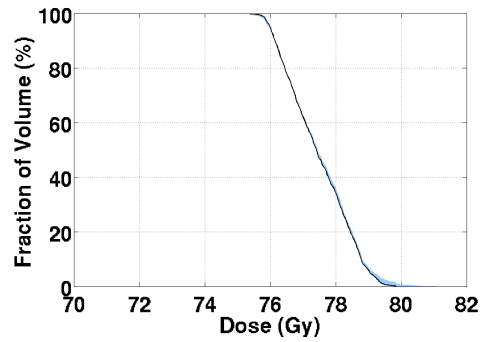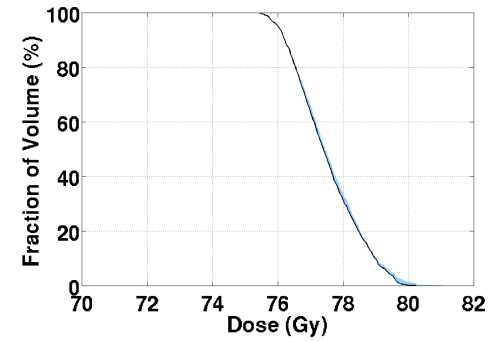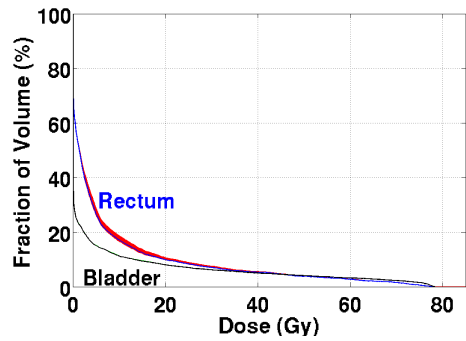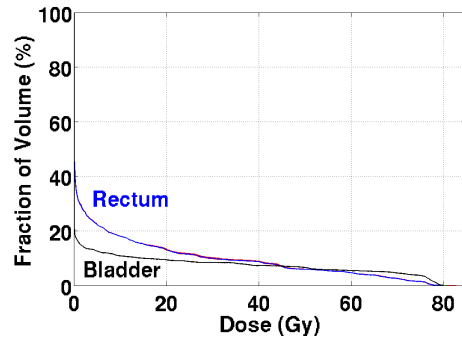
Figure 1: Dose-volume histogram (DVH) bands for target dose distributions covering all setup uncertainties for the organs at risk (the rectum and bladder) resulting from the deterministic approach (a), CCP under the normality assumption (CCP-N; b), and CCP under the uniformity assumption (CCP-U; c). The width of the DVH band is inversely proportional to the robustness of the method. The solid lines indicate DVHs for the nominal dose distribution (i.e., without consideration of uncertainties).
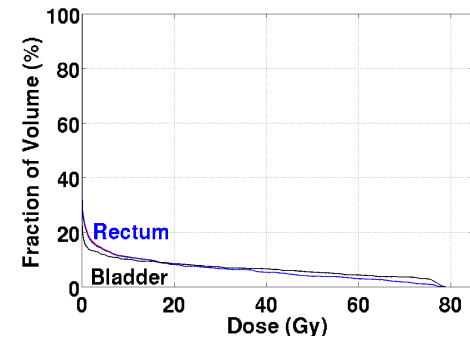


Figure 2: Dose-volume histogram (DVH) bands for dose distributions to organs at risk covering all setup uncertainties for the target volume, resulting from the deterministic approach (a), CCP under the normality assumption (CCP-N; b), and CCP under the uniformity assumption (CCP-U; c). The width of the DVH band is inversely proportional to the robustness of the method. The solid lines indicate DVHs for the nominal dose distribution (i.e., without consideration of uncertainties).
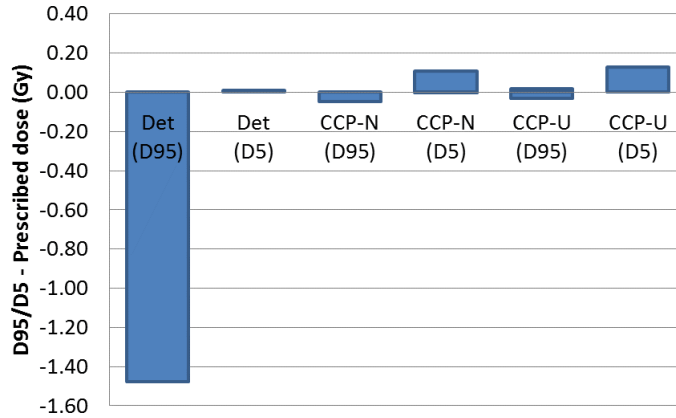
Figure 3: $D_{95}$ or $D_5$ minus prescribed dose from deterministic (Det), CCP-N, and CCP-U models under random setup scenarios. The height of the boxes shows the band width, i.e., $\Delta(D_{95})$ in the DVH family of setup errors. The larger the band width, the less robustness in dose distribution.

To further evaluate the robustness of IMRT plans for target coverage, DVH family band widths from six models were compared using two key dose-volume indices of target coverage, $D_{95}$ and $D_5$. $D_{95}$ is a measure to assess target coverage, and $D_5$ is used to assess hot spots on the target. Figure 3 compares the deterministic, CCP-N, and CCP-U models in controlling the robustness of target coverage under uncertainty. The band widths for $D_5$ show that the deterministic model better controlled hot spots on the target than did the CCP models: the second bar is smaller than the fourth and sixth bars, which correspond to the CCP-N and CCP-U models, respectively. However, the band widths for $D_{95}$ show that the CCP models controlled the cold spots under uncertainties much better than did the deterministic model; the band widths corresponding to the CCP models (third and fifth bars) are much smaller than that of the deterministic model (first bar). Similarly, Figure 1 demonstrates that the radiation dose (x-axis) received by 95% of target voxels (y-axis) was much closer to the 76 Gy prescribed dose for the CCP models. It should be noted that avoiding cold spots on the target is generally a higher priority in clinical practice that avoiding hot spots. Dose-volume indices of OARs and the corresponding DVH family band widths are not shown in Figure 3 because the OAR sparing and the corresponding robustness of all three methods were similar, as shown in Figures 1 and 2.

*4.3. Discussions related to robust optimization*

An inter-comparison of the dose coverage of IMRT plans using CCP and those using robust optimization is discussed in this section. The worst-case dose robust optimization method was utilized by substituting the worst-case dose distribution for the nominal dose. To form the worst-case dose distribution, for a voxel inside the target, the minimum dose to this voxel from all dose distributions corresponding to a range of uncertainty scenarios was selected, and for any voxels outside the target, the maximum dose of the voxel was selected.

The robust optimization was performed assuming a maximum of setup error scenario ($\pm 5\,mm$). Then, the robustness of the robustly optimized plans was evaluated under maximum setup errors of both $\pm 5\,mm$ and $\pm 7.5\,mm$. To ensure a fair comparison between the robustly optimized plans and the chance-constrained plans, we also evaluated the robustness of IMRT plans generated using CCP models for maximum setup errors of both $\pm 5\,mm$ and $\pm 7.5\,mm$. The corresponding DVH family bands for the target derived from the robust optimization and two CCP methods are illustrated in Figure 4.

Figure 4a represents the DVH family band from robustly optimized plans that were evaluated for the same uncertainty set as that considered in the robust optimization. In this figure, the nominal plan (black line) was more homogeneous than were the nominal CCP plans (black lines in Figures 4b and 4c), and the target was robustly covered, as indicated by the narrow DVH family band (shaded area). However, when we assumed that uncertainties may occur to a greater extent and therefore evaluated the robustness of the same plan for a wider range of setup scenarios (up to $\pm 7.5\,mm$), the target coverage was not as robust as before. As shown in Figure 4d, the DVH band from a robustly optimized plan evaluated for a maximum shift of $\pm 7.5\,mm$ was wider than the band of the same plan evaluated for a maximum shift of $\pm 5\,mm$ (Figure 4a). More specifically, there were a lot more cold spots on the target when uncertainties were in a wider range, which is not acceptable in clinical practice. This situation arises as a result of the underlying assumption behind the robust optimization method: that the real uncertainty set is well defined and contains the uncertainty scenarios. In reality, this assumption is flawed, so the robustly optimized plan might not be robust in the face of real uncertainties.

However, the DVH family bands were much narrower in Figures 4e and 4f than in Figure 4d, indicating that the target coverage of IMRT dose distributions generated by the CCP-N and CCP-U models was more robust than that of the robustly optimized plan for setup errors in the $\pm 5\,mm$ and $\pm 7.5\,mm$ maximum range.
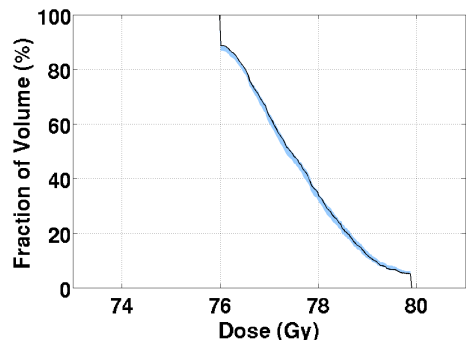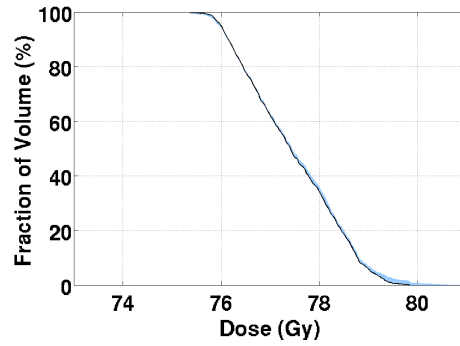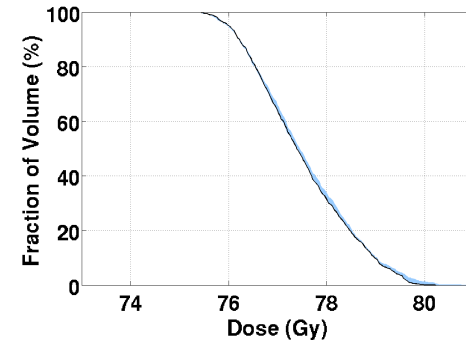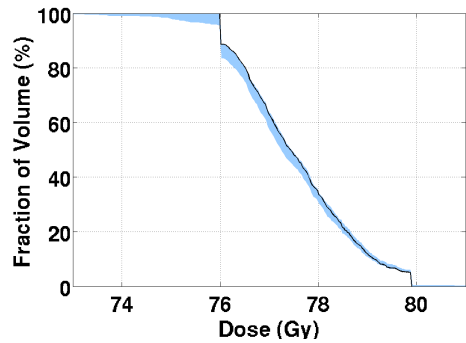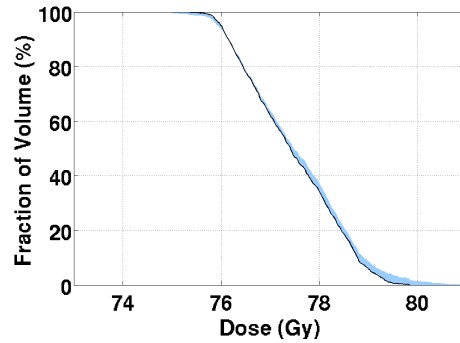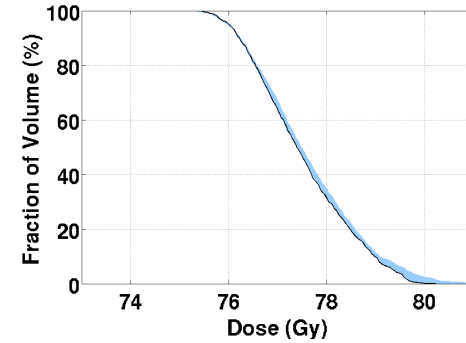
Figure 4: Dose-volume histogram (DVH) bands for dose distributions covering all setup uncertainties for the target volume, resulting from robust optimization (RO; left column), CCP under the normality assumption (CCP-N; center column), and CCP under the uniformity assumption (CCP-U; right column). The robustness of the plans was evaluated for two setup uncertainty ranges, up to $\pm 5\,mm$ and $\pm 7.5\,mm$ in the top and bottom rows, respectively. The width of the DVH band is inversely proportional to the robustness of the method. The solid lines indicate DVHs for the nominal dose distribution (i.e., without consideration of uncertainties).

*4.4. Confidence levels*

In probabilistic approaches such as CCP-N (I) and CCP-U (I), solutions can be provided using the statistical confidence levels associated with the probabilities of satisfaction for constraints. When these confidence levels are treated as variables, the corresponding optimal levels of confidence can be achieved based on a planner's preference on fixed values of hot-spot ($\theta_U$) and cold-spot ($\theta_L$) control parameters on the target and of the hot-spot control parameter on the OAR ($\varphi$) in the optimization model. Ultimately, a planner can use this method to generate a treatment plan with an acceptable confidence level. Table 2 shows the optimized confidence levels for two choices of control parameters ($\theta_L$ and $\theta_U$) in the CCP-N (I) and CCP-U (I) models.

Table 2: Confidence levels $(1 - \alpha)$ of the plans generated by CCP models

(a) Tight bounds

| Model | Target | | Rectum | Bladder |
|---|---|---|---|---|
| | Under-dose | Over-dose | | |
| CCP-N (I) | 0.93 | 0.93 | 1 | 1 |
| CCP-U (I) | 0.85 | 0.85 | 0.88 | 0.84 |

(b) Loose bounds
1% decrease in lower bound ($\theta_L$) and 2% increase in upper bounds ($\theta_U$ and $\varphi$)

| Model | Target | | Rectum | Bladder |
|---|---|---|---|---|
| | Under-dose | Over-dose | | |
| CCP-N (I) | 1 | 1 | 1 | 1 |
| CCP-U (I) | 0.92 | 0.94 | 0.93 | 0.93 |

In a chance-constrained setting, the constraints are not expected to hold with a lower probability when the hot-spot control parameters ($\theta_U$ and $\varphi$) are increased or the cold-spot control parameter ($\theta_L$) is decreased. This characteristic of the CCP approach was verified, and the results are shown in Tables 2a and 2b for tight and loose ranges of control parameters, respectively. Comparing the first rows of Tables 2a and 2b, which correspond to the CCP-N (I) model, all confidence levels either increased or remained the same when looser bounds were used (Table 2b). The confidence levels for target constraints increased from 0.93 using tight bounds to 1 using loose bounds, and the confidence levels corresponding to rectum and bladder remained the same. Similarly, the results of the CCP-U (I) model are compared in the second rows of Tables 2a and 2b. The confidence levels for satisfaction of the target constraints increased from 0.85 using tight bounds to 0.92 for

under-dose and 0.94 for over-dose using loose bounds. For OARs, the confidence levels increased from 0.88 for rectum and 0.84 for bladder with tight bounds to 0.93 with loose bounds. Hence, the confidence levels for satisfaction of the loosely bounded constraints (Table 2b) were consistently equal to or higher than the corresponding confidence levels for more tightly bounded constraints (Table 2a).

## 4.5. Optimized bounds

It is always helpful to know what probability of satisfaction for clinical constraints under uncertainty is guaranteed. A high confidence level for the satisfaction of the treatment planning constraints is desirable in radiation therapy treatment planning, as in any optimization problem. The proposed models CCP-N (II) and CCP-U (II) ensure the feasibility of the constraints by optimizing the hot- and cold-spot control parameters.

Table 3: Cold- and hot-spot control parameters ($\theta_L$ and $\theta_U$) optimized by the CCP-N (II) model for four different penalty coefficient ($\lambda$) settings (95% confidence level)

| $\lambda_T^-, \lambda_T^+$ | $\underline{\theta}_L = 0.97, \bar{\theta}_L = 1$ $\underline{\theta}_U = 1, \bar{\theta}_U = 1.1$ | | $\underline{\theta}_L = 0.95, \bar{\theta}_L = 1$ $\underline{\theta}_U = 1, \bar{\theta}_U = 1.1$ | | $\underline{\theta}_L = 0.9, \bar{\theta}_L = 1$ $\underline{\theta}_U = 1, \bar{\theta}_U = 1.15$ | |
|---|---|---|---|---|---|---|
| | $\theta_L$ | $\theta_U$ | $\theta_L$ | $\theta_U$ | $\theta_L$ | $\theta_U$ |
| 1, 1 | 0.97 | 1.048 | 0.95 | 1.026 | 0.9 | 1 |
| 10, 1 | 1 | 1.08 | 1 | 1.08 | 1 | 1.08 |
| 1, 10 | 0.97 | 1.042 | 0.95 | 1.021 | 0.9 | 1 |
| 10, 10 | 0.97 | 1.042 | 0.95 | 1.021 | 0.93 | 1 |

Before verifying that the models behave in the way expected, we explored the proper values for penalty coefficients in the objective function. Thus, four different settings for penalty coefficients ($\lambda$) were used, and the corresponding optimal cold- and hot-spot control parameters for the target are shown in Tables 3 and 4 for the CCP-N (II) and CCP-U (II) models, respectively. The columns in Tables 3 and 4 correspond to three different settings of lower and upper bounds on $\theta_L$ and $\theta_U$, while the confidence levels are fixed to 95% and 90% for the CCP-N (II) and CCP-U (II) models, respectively.

As presented in the second row of Tables 3 and 4, imposing a larger penalty on cold spots resulted in increasing the cold-spot control parameter ($\theta_L$) to avoid cold spots on the target. Similarly, a higher penalty on the hot spots resulted in a smaller hot-spot control parameter ($\theta_U$), as shown in the third rows of Tables 3 and 4. For the remainder of the

Table 4: Cold- and hot-spot control parameters ($\theta_L$ and $\theta_U$) optimized by the CCP-U (II) model for four different penalty coefficient ($\lambda$) settings (90% confidence level)

| $\lambda_T^-, \lambda_T^+$ | $\underline{\theta}_L = 0.97, \bar{\theta}_L = 1$ $\underline{\theta}_U = 1, \bar{\theta}_U = 1.15$ | | $\underline{\theta}_L = 0.95, \bar{\theta}_L = 1$ $\underline{\theta}_U = 1, \bar{\theta}_U = 1.15$ | | $\underline{\theta}_L = 0.9, \bar{\theta}_L = 1$ $\underline{\theta}_U = 1, \bar{\theta}_U = 1.15$ | |
|---|---|---|---|---|---|---|
| | $\theta_L$ | $\theta_U$ | $\theta_L$ | $\theta_U$ | $\theta_L$ | $\theta_U$ |
| 1 ,1 | 0.97 | 1.101 | 0.95 | 1.079 | 0.9 | 1.022 |
| 10, 1 | 1 | 1.135 | 1 | 1.135 | 1 | 1.135 |
| 1,10 | 0.97 | 1.097 | 0.95 | 1.074 | 0.9 | 1.018 |
| 10,10 | 0.97 | 1.097 | 0.95 | 1.074 | 0.9 | 1.018 |

experiments in this section, both penalty coefficient parameters $\lambda_T^-$ and $\lambda_T^+$ were set to 10 on the basis of these trials.

Next, the confidence levels were changed, and for each specified level of confidence, the bounds of the constraints were optimized using models CCP-N (II) and CCP-U (II). Tables 5 and 6 illustrate the results for three different levels of confidence for each of the models, CCP-N (II) and CCP-U (II), respectively. In addition, for each confidence level, three different settings of lower and upper bounds on $\theta_L$ and $\theta_U$ were analyzed; these are shown in three columns in Tables 5 and 6. It was also assumed that the confidence level for the rectum and bladder was fixed to 95% and 90% for the CCP-N (II) and CCP-U (II) models, respectively.

For both models, it is consistently demonstrated that if the treatment planner intends to meet the constraints with higher confidence in the face of randomness, the bounds on the constraints must either remain the same or be loosened. For example, in Table 5, as the confidence level increases by moving down the rows, the cold-spot control parameter $\theta_L$ remains constant in the first and second columns and decreases in the third. As a result, we can conclude that when the confidence level is increased, the lower boundaries on the constraints either remain the same or become smaller. On the other hand, $\theta_U$ increases in the first and second columns and remains the same in the third column. Similarly, increasing the expected level of confidence on the satisfaction of the constraints does not tighten the upper bounds of the constraints. Table 6 can be discussed in a similar fashion. As a result, considering models CCP-N (II) and CCP-U(II) will allow the treatment planner to better choose between different choices of treatment plan.

25

Table 5: Target constraint bounds ($\theta_L$ and $\theta_U$) of the plans generated by the CCP-N (II) model for different confidence levels (95% confidence level for OARs)

| $1-\alpha_T$ | $\underline{\theta}_L = 0.97, \bar{\theta}_L = 1$ $\underline{\theta}_U = 1, \bar{\theta}_U = 1.1$ | | $\underline{\theta}_L = 0.95, \bar{\theta}_L = 1$ $\underline{\theta}_U = 1, \bar{\theta}_U = 1.1$ | | $\underline{\theta}_L = 0.9, \bar{\theta}_L = 1$ $\underline{\theta}_U = 1, \bar{\theta}_U = 1.15$ | |
|---|---|---|---|---|---|---|
| | $\theta_L$ | $\theta_U$ | $\theta_L$ | $\theta_U$ | $\theta_L$ | $\theta_U$ |
| 0.935 | 0.97 | 1.039 | 0.95 | 1.018 | 0.933 | 1 |
| 0.95 | 0.97 | 1.042 | 0.95 | 1.021 | 0.93 | 1 |
| 0.97 | 0.97 | 1.048 | 0.95 | 1.027 | 0.925 | 1 |

Table 6: Target constraint bounds ($\theta_L$ and $\theta_U$) of the plans generated by the CCP-U (II) model for different confidence levels (90% confidence level for OARs)

| $1-\alpha_T$ | $\underline{\theta}_L = 0.97, \bar{\theta}_L = 1$ $\underline{\theta}_U = 1, \bar{\theta}_U = 1.15$ | | $\underline{\theta}_L = 0.95, \bar{\theta}_L = 1$ $\underline{\theta}_U = 1, \bar{\theta}_U = 1.15$ | | $\underline{\theta}_L = 0.9, \bar{\theta}_L = 1$ $\underline{\theta}_U = 1, \bar{\theta}_U = 1.15$ | |
|---|---|---|---|---|---|---|
| | $\theta_L$ | $\theta_U$ | $\theta_L$ | $\theta_U$ | $\theta_L$ | $\theta_U$ |
| 0.86 | 0.97 | 1.082 | 0.95 | 1.06 | 0.9 | 1.004 |
| 0.88 | 0.97 | 1.089 | 0.95 | 1.066 | 0.9 | 1.01 |
| 0.9 | 0.97 | 1.097 | 0.95 | 1.074 | 0.9 | 1.018 |

## 5. Conclusion

The inclusion of uncertainties in radiation therapy treatment planning has been widely recognized as essential. We found CCP to be an effective approach to controlling uncertainties in treatment planning optimization. The proposed stochastic programming framework optimizes the quality, robustness, and homogeneity of the plans as well as the confidence level of the constraints in the face of patient setup uncertainties. Depending on the assumptions that we made regarding the probability distribution of random dose contributions, two different sets of deterministic equivalents of the treatment planning chance constraints developed. Then, for each set of deterministic counterparts, two CCP optimization models were explored to optimize either the confidence or homogeneity of the plans, according to the treatment planner's preference. All proposed CCP models were tested using data for a real prostate cancer patient and shown to more efficiently control uncertainties in treatment planning optimization than did a deterministic approach.As a future study, the CCP model could be extended for the case when partial information on the probability distribution, such as mean and variance, is available.

## Bibliography

American Cancer Society. (2015). "Cancer facts & figures." *Retrieved from http://www.cancer.org/research/cancerfactsfigures/acspc-031941*.

An, Y., Liang, J., Schild, S. E., Bues, M., & Liu, W. (2017). "Robust treatment planning with conditional value at risk chance constraints in intensitymodulated proton therapy." *Medical physics*, 44(1), 28–36.

Baum, C., Alber, M., Birkner, M., & Nüsslin, F. (2006). "Robust treatment planning for intensity modulated radiotherapy of prostate cancer based on coverage probabilities." *Radiotherapy and Oncology*, 78(1), 27–35.

Bazaraa, M. S., Sherali, H. D., & Shetty, C. M. (2013). "Nonlinear programming: theory and algorithms." Hoboken, NJ: John Wiley & Sons.

Bertsimas, D., & Popescu, I. (2005). "Optimal inequalities in probability theory: a convex optimization approach." *SIAM Journal on Optimization*, 15(3), 780–804.

Birge, J. R., & Louveaux, F. (2011). "Introduction to stochastic programming." New York: Springer Science & Business Media.

Calafiore, G. C., & El Ghaoui, L. (2006). "On distributionally robust chance-constrained linear programs." *Journal of Optimization Theory and Applications*, 130(1), 1–22.

Cao, W., Lim, G. J., Lee, A, Li, Y, Liu, W, Zhu, X. R., & Zhangårdemark, X. (2012). "Uncertainty incorporated beam angle optimization for IMPT treatment planning." *Medical Physics*, 39(8), 5248–5256.

Cao, W., Lim, G. J., Li, X., Li, Y., Zhu, X. R., & Zhang, X. (2013). "Incorporating deliverable monitor unit constraints into spot intensity optimization in intensity-modulated proton therapy treatment planning." *Physics in Medicine and Biology*, 58(15), 5113–5125.

Cao, W., Lim, G., Liao, L., Li, Y., Jiang, S., Li, X., ... & Zhang, X. (2014). "Proton energy optimization and reduction for intensity-modulated proton therapy." *Physics in Medicine and Biology*, 59(21), 6341–6354.

Chan, T. C., Tsitsiklis, J. N., & Bortfeld, T. (2010). "Optimal margin and edge-enhanced intensity maps in the presence of motion and uncertainty." *Physics in Medicine and Biology*, 55(2), 515–533.

Chan, T. C., & Mišić, V. V. (2013). "Adaptive and robust radiation therapy optimization for lung cancer." *European Journal of Operational Research*, 231(3), 745–756.

Charnes, A., & Cooper, W. W. (1959). "Chance-constrained programming." *Management Science*, 6(1), 73–79.

Charnes, A., & Cooper, W. W. (1963). "Deterministic equivalents for optimizing and satisficing under chance constraints." *Operations Research*, 11(1), 18–39.

Chu, M., Zinchenko, Y., Henderson, S. G., & Sharpe, M. B. (2005). "Robust optimization for intensity modulated radiation therapy treatment planning under uncertainty." *Physics in Medicine and Biology*, 50(23), 5463–5477.

Drzymala, R. E., Mohan, R., Brewster, L., Chu, J., Goitein, M., Harms, W., & Urie, M. (1991). "Dose-volume histograms." *International Journal of Radiation Oncology\* Biology\* Physics*, 21(1), 71–78.

Fredriksson, A., Forsgren, A., & Hårdemark, B. (2011). "Minimax optimization for handling range and setup uncertainties in proton therapy." *Medical Physics*, 38(3), 1672–1684.

Fredriksson, A., Forsgren, A., & Hårdemark, B. (2015). "Maximizing the probability of satisfying the clinical goals in radiation therapy treatment planning under setup uncertainty." *Medical Physics*, 42(7), 3992–3999.

Geletu, A., Klöppel, M., Zhang, H., & Li, P. (2013). "Advances and applications of chance-constrained approaches to systems optimization under uncertainty." *International Journal of Systems Science*, 44(7), 1209–1232.

Henrion, R., & Möller, A. (2012). "A gradient formula for linear chance constraints under Gaussian distribution." *Mathematics of Operations Research*, 37(3), 475–488.

Hoeffding, W. (1963). "Probability inequalities for sums of bounded random variables." *Journal of the American Statistical Association*, 58(301), 13–30.

Kali, P., & Wallace, S. W. (1994). "Stochastic programming." New York: Springer.

Lagoa, C. M., Li, X., & Sznaier, M. (2005). "Probabilistically constrained linear programs and risk-adjusted controller design." *SIAM Journal on Optimization*, 15(3), 938–951.

Li, P., Arellano-Garcia, H., & Wozny, G. (2008). "Chance-constrained programming approach to process optimization under uncertainty." *Computers & Chemical Engineering*, 32(1), 25–945.

Lim, G. J., Choi, J., & Mohan, R. (2008). "Iterative solution methods for beam angle and fluence map optimization in intensity modulated radiation therapy planning." *OR Spectrum*, 30(2), 289–309.

Lim, G. J., & Cao, W. (2012). "A two-phase method for selecting IMRT treatment beam angles: branch-and-prune and local neighborhood search." *European Journal of Operational Research*, 217(3), 609–618.

Liu, W., Li, Y., Li, X., Cao, W., & Zhangårdemark, X. (2012). "Influence of robust optimization in intensity-modulated proton therapy with different dose delivery techniques." *Medical Physics*, 39(6), 3089-3101.

Liu, W., Zhang, X., Li, Y., & Mohan, R. (2012) "Robust optimization of intensity modulated proton therapy." *Medical Physics* 39(2): 1079–1091.

Lomax, A. J., Boehringer, T., Coray, A., Egger, E., Goitein, G., Grossmann, M., ... & Roser, W.

(2001). "Intensity modulated proton therapy: a clinical example." *Medical Physics*, 28(3), 317–324.

Narkiss, G., & Zibulevsky, M. (2005). "Sequential subspace optimization method for large-scale unconstrained problems." *(CCIT Report #559). Haifa, Israel: Technion-Israel Institute of Technology, Department of Electrical Engineering.*

Nemirovski, A., & Shapiro, A. (2006). "Convex approximations of chance-constrained programs." *SIAM Journal on Optimization*, 17(4), 969–996.

Olafsson, A., & Wright, S. (2006). "Efficient schemes for robust IMRT treatment planning." *Physics in Medicine and Biology*, 51(21), 5621–5642.

Pflugfelder, D., Wilkens, J., & Oelfke, U. (2008). "Worst case optimization: a method to account for uncertainties in the optimization of intensity modulated proton therapy." *Physics in Medicine and Biology*, 53(6), 1689.

Pintér, J. (1989). "Deterministic approximations of probability inequalities." *Zeitschrift für Operations Research*, 33(4), 219–239.

Prékopa, A. (1986). "Stochastic programming 84." New York: Springer.

Prékopa, A. (1995) "Stochastic programming." New York: Springer.

Reemtsen, R., & Alber, M. (2009). "Continuous optimization of beamlet intensities for photon and proton radiotherapy." *In P. M. Pardalos & H. E. Romeijin (Eds.), Handbook of Optimization in Medicine* (pp. 1–40). New York: Springer.

Siegel, R. L., Miller, K. D., Fedewa, S. A., Ahnen, D. J., Meester, R. G., Barzi, A., & Jemal, A. (2017). "Colorectal cancer statistics." *A Cancer Journal for Clinicians*, 67(3), 177–193.

Trofimov, A., Unkelbach, J., Delaney, T. F., & Bortfeld, T. (2012). "Visualization of a variety of possible dosimetric outcomes in radiation therapy using dose-volume histogram bands." *Practical Radiation Oncology*, 2(3), 164–171.

Zelefsky, M. J., Fuks, Z., Happersett, L., Lee, H. J., Ling, C. C., Burman, C. M., ... & Skwarchuk, M. (2000). "Clinical experience with intensity modulated radiation therapy (IMRT) in prostate cancer." *Radiotherapy and Oncology*, 55(3), 241–249.